

A Non-Invasive Gait-Based Screening Approach for Parkinson's Disease

Chen Hui^a, Tee Connie^{a,*}, Michael Kah Ong Goh^a, Nor 'Izzati binti Saedon^b

^a Faculty of Information Science and Technology, Multimedia University, Jalan Ayer Keroh Lama, 75450, Melaka, Malaysia

^b Department of Medicine, Faculty of Medicine, Universiti Malaya, 50603, Kuala Lumpur, Malaysia

Corresponding author: *tee.connie@mmu.edu.my

Abstract— Parkinson's disease (PD) presents a significant global health challenge, characterized by the progressive degeneration of dopamine-producing neurons in the brain, resulting in both motor and non-motor symptoms that severely impact quality of life. This study addresses the complexities of PD, highlighting the critical need for early diagnosis to slow disease progression. This research addresses the challenges of early diagnosis, such as the use of unreliable diagnostic techniques and limited healthcare resources. It uses the MMU Parkinson Disease Dataset and applies camera-based data collection to analyze gait patterns that can identify a risk of Parkinson's Disease. The study utilizes computer vision and the AlphaPose framework to analyze video data and detect body key points. By employing machine learning algorithms, including Support Vector Machines (SVM) and CatBoost, showing highly effective in identifying temporal dependencies in gait patterns. The algorithms achieved a high accuracy of 83.33% on the MMU dataset. This method enhances the accuracy of PD detection and enables immediate detection and control of the disease. The combination of advanced data analysis methods and medical knowledge offers new possibilities to develop targeted treatments that improve patient outcomes, demonstrating the potential of machine learning in effectively managing and treating Parkinson's disease. To enhance the generalizability of models, future research should collect extensive and diverse datasets covering various backgrounds and different stages of Parkinson's disease and utilize advanced techniques for extracting features to improve the accuracy of gait analysis.

Keywords— Parkinson's disease; computer vision; AlphaPose; machine learning; gait features.

Manuscript received 15 Dec. 2023; revised 19 Mar. 2024; accepted 21 Jul. 2024. Date of publication 31 Oct. 2024.
IJASEIT is licensed under a Creative Commons Attribution-Share Alike 4.0 International License.



I. INTRODUCTION

Parkinson's disease (PD) is a global disease that gradually affects individuals, families, and healthcare systems. It is caused by the degeneration of dopamine-producing neurons in the brain, resulting in motor symptoms such as tremors, bradykinesia, stiffness, and posture instability. In addition, PD includes non-motor symptoms such as mental health disorders and memory problems, which further complicate the treatment and delivery of medical care.

With a growing number of PD cases, it is crucial for public health efforts to prioritize the comprehension, diagnosis, and treatment of this complicated condition [1]. A thorough assessment of Parkinson's disease (PD), including physical and non-physical symptoms, is essential. Early diagnosis is essential, as PD develops gradually and can go undetected for years without showing symptoms [2]. Detecting the disease early can lead to timely treatment, potentially slowing its progression and alleviating symptoms.

However, several challenges hinder early diagnosis. The lack of reliable diagnostic tools makes early detection easier, leading to delayed treatment and poorer outcomes. Additionally, limited healthcare resources, such as a shortage of neurologists and specialized clinics, result in long waits for diagnosis and treatment. The high costs of advanced diagnostic technologies also limit access to prompt diagnosis and care.

This study proposes a cost-effective solution that uses camera-based data to analyze walking patterns as potential indicators of PD. The aim is to identify specific gait features that could be signs of the disease. The study computes gait features that characterize walking patterns by employing computer vision techniques to detect human body key points in video footage. Machine learning algorithms are then used to classify these patterns associated with PD. This proposed system aims to improve real-world applications in the early detection and monitoring of Parkinson's disease.

II. MATERIALS AND METHOD

A. Literature Review

Understanding the movement characteristics of PD patients is crucial for predicting and managing the illness. This section presents related work on applying machine learning to PD prediction.

1) Conventional Methods:

In 2022, Escamilla-Luna et al. [3] conducted a detailed analysis by extracting 56 gait characteristics from accelerometer data attached to each patient's left and right ankles, using the "iGAIT" tool in MATLAB. They measured 28 variables per accelerometer, encompassing spatiotemporal features, frequency domain metrics, and the regularity/symmetry of step movements. The accelerometers tracked vertical movement (Y-axis), anterior-posterior movement (X-axis), and middle-lateral movement (Z-axis), which correlated with different aspects of gait. This thorough feature extraction allowed for an in-depth analysis of gait dynamics and their relationship to Parkinson's disease.

Ajay et al. [4] focused on assessing shuffling steps, slow gait, gait asymmetry, knee and ankle positions, and head position using video frame data. Shuffling steps were identified by measuring reduced ankle displacement during the double support phase, producing a feature called *fstep-shuffle*. Slow gait was detected by comparing the frequency of double support detections to the normal healthy cycle time, resulting in the feature *fslow-gait*. Gait asymmetry, often caused by Freezing-of-Gait, was quantified by comparing ankle displacement amplitudes between the right and left limbs during double support, creating the *step-asym* feature (*fstep-asym*). These methods provided valuable tools for analyzing and understanding the unique gait patterns associated with Parkinson's disease.

Urcuqui et al. [5] employed the e-Motion Capture System with Kinect technology to measure body distances as participants moved in a 1.5 x 4-meter corridor. Using wavelet methods and the Daubechies wavelet (db8), they identified gait phases and generated spatiotemporal variables to differentiate individuals with PD. This approach highlighted the relationship between gait phases and signals, facilitating the computation of spatiotemporal characteristics. The study focused solely on gait analysis, excluding participants with specific medical and psychiatric disorders.

Liu et al. [6] analyzed hand movements by extracting features from sequences of hand joint locations over time. They measured periodic patterns of hand motions, including finger tapping, hand clasping, and hand supination, emphasizing the alternating rise and drop within a single movement course. An extrema extraction method was used in the finger-tapping task to characterize motor abnormalities during hand motions. Similar techniques were applied to other activities to provide insights into motor dysfunction based on hand joint positions over time.

Seo et al. [7] used the Short-Time Auto Correlation Function (ST-ACF) to extract enhanced-resolution movement features. They applied Dynamic Time Warping (DTW) to identify PD individuals with varying gait speeds, particularly those with freezing symptoms or tracking errors. This approach offered a robust method for analyzing and

identifying unique movement patterns associated with Parkinson's disease. DTW produced a time-course of waveform distances at 10-interval intervals throughout each walking sequence by comparing ST-ACF waveforms at each lag to an average "healthy" waveform from the CASIA dataset. This long-distance time-course included a component that strengthened the movement pattern analysis's resilience in the face of changes in gait speed or other influencing variables seen in PD patients. A summary of the conventional methods is provided in Table I.

TABLE I
A SUMMARY OF CONVENTIONAL METHODS

Author	Method	Dataset	Data Characteristics	Accuracy
Escamilla-Luna et al. [3]	SVM	Self-collected dataset	Change of velocity	97.5%
Ajay et al. [4]	Binary decision tree	YouTube videos	Gait in PD	93.75%
Urcuqui et al. [5]	RF, LR, NB	Self-collected dataset	Gait in PD	RF: 82%, NB: 64%, LR: 76%
Liu et al. [6]	RF, KNN, L-SVM, RBF-SVM	MPII dataset	Hand movements in PD	KNN: 72.7%, RF: 80.4%, L-SVM: 83.5%, RDF-SVM: 89.7%
Seo et al. [7]	Neural Network, SVM, Ensemble classifier	CASIA dataset	Arms and leg joints movements in PD	Neural Network: 93%, SVM: 92%, Ensemble classifier: 97%

2) Deep Learning:

In 2021, Balaji et al. [8] extracted gait features from the gait cycle to discriminate between healthy and PD patients using the LSTM model. The two primary stages of the gait cycle were the swing and stance phases, representing 60% and 40% of the overall gait cycle. Capturing these spatiotemporal aspects with VGRF sensors assisted in finding the essential biomarkers for successful classifications.

Prince and De Vos [9] extracted gait features for PD classification using traditional machine learning techniques and deep learning approaches. For the tapping test, 13 spatiotemporal elements were derived from pixel coordinate data, including speed, rhythm, accuracy, and fatigue. Besides, 28 characteristics were retrieved from frequency and temporal domains from each accelerometer waveform. The extracted features were concatenated to generate the manual feature set X_m , utilized for classification.

Li et al. [10] extracted features from Timed Up and Go (TUG) video sequences taken with a 2D camera in a controlled situation. The approach automatically separated the video into six sub-tasks: 'Sit,' 'Sit-to-Stand,' 'Walk,' 'Turn,' 'Walk-Back,' and 'Sit-Back'. The approach involved employing a human pose estimator to obtain key point

coordinates from the video frames. These coordinates were spatially adjusted to prepare them for analysis. Next, the normalized features from consecutive frames were concatenated to capture spatial and temporal information. Using the concatenated feature sequences, a classifier was applied to predict the sub-task categorization on a frame-by-frame basis. DTW was used to improve the sub-task segmentation by using the frame-wise predictions from the classifier. This method allows for precise division and analysis of several phases.

Reyes et al. [11] used a one-dimensional convolutional neural network (1D CNN) to extract features from time signal data automatically. Employing a temporal frame (kernel) could analyze parts of the signals to identify problems independently. The improved model design consisted of three consecutive 1D convolutional layers with max pooling for down-sampling. The model concluded with an output layer that used a sigmoid function and the Adam optimizer. They employed learning rate scheduling to enhance convergence and accelerate the learning process.

Hssayeni et al. [12] developed a deep learning method that uses Long Short-Term Memory (LSTM) networks to evaluate the medication conditions of people with Parkinson's disease using wearable sensors. The system was evaluated on two datasets, showing encouraging classification rates. Dataset 1 had an average accuracy of 73%, while Dataset 2 achieved an average accuracy of 77%. The study emphasized the potential effectiveness of deep learning algorithms in precisely identifying medication updates in persons with Parkinson's disease. A summary of the deep learning methods is presented in Table II.

TABLE II
A SUMMARY OF DEEP LEARNING METHODS

Author	Method	Dataset	Data Characteristics	Accuracy
Balaji et al. [8]	Long short-term memory (LSTM)	Vertical ground reaction force (VGRF) dataset	Gait in Parkinson's disease	Multi-class: 96.60% Binary: 98.60%
Prince & De Vos [9]	DNN, CNN	Self-collected dataset	Gait in Parkinson disease	DNN: 61.2% CNN: 62.1%
Li et al. [10]	LSTM, SVM	Self-collected dataset	Gait in Parkinson disease	I + S: 91.9% I + L: 92.7% O + S: 92.8% O + L: 93.1%
Reyes et al. [11]	LSTM, Conv1D, Conv LSTM	Self-collected dataset	Gait in Parkinson disease	LSTM: 53%, Conv1D: 82%, Conv LSTM: 83.1%
Hssayeni et al. [12]	LSTM	Self-collected dataset	Gait in Parkinson disease	73%

B. Proposed Solution

This section summarizes the basic processes employed in this study to identify and predict Parkinson's disease (PD). As shown in Fig. 1, the workflow includes eight key steps: 1) Data Collection, 2) Video Enhancement, 3) Body Key-Point Estimation, 4) Gait Signal Pre-processing, 5) Turning Frames Extraction, 6) Gait Cycle Identification, 7) Feature Extraction, and 8) Classification.

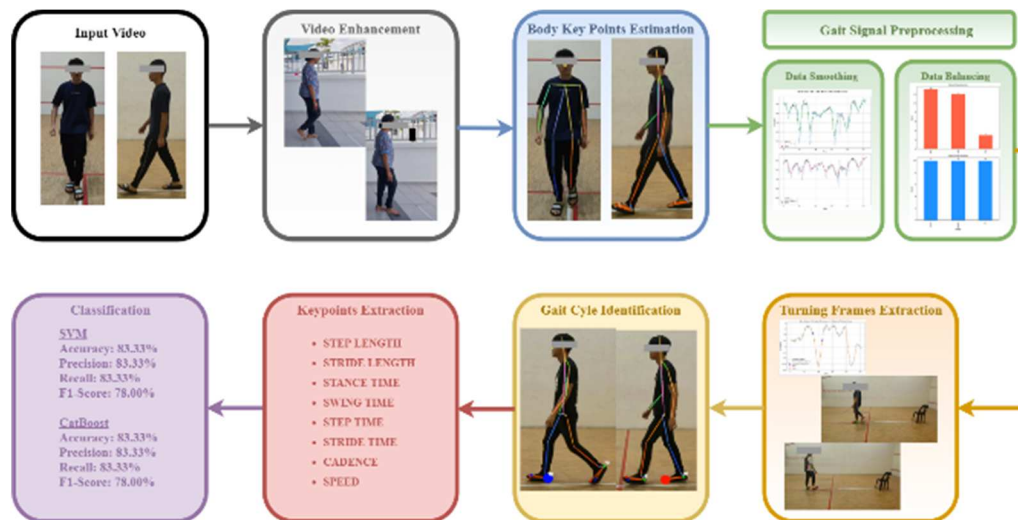


Fig. 1 Flowchart of PD recognition system.

First, videos are recorded to gather the gait data. Next, the body key points are extracted from these videos. Following that, a filtering method is implemented to improve the quality of the collected data. The enhanced data is then used to determine specific gait features. At last, these extracted features are used in the classification stage to differentiate between PD patients and healthy individuals.

1) Data Collection:

Data collection is a crucial part of this research project, focusing on collecting complete information on patient

characteristics, medical histories, and results derived from the Timed Up and Go (TUG) test [13]. This section explains the processes used for collecting and processing data.

Firstly, all participants, including healthy individuals and PD patients, must provide informed consent. Participants are provided with a comprehensive consent form outlining the research objectives and methodologies employed and highlighting participation's voluntary aspect. Potential participants can inquire about any concerns and express their reservations before agreeing to participate in the research.

Next, participants are instructed to do the Timed Up and Go (TUG) test under guidance. The participants are given detailed instructions to ensure their complete comprehension of the testing procedure, which involves rising from a seated position, walking 3 meters, turning, returning to the chair, and getting a seated position [14]. Fig. 2 and Fig. 3 show the setup of the TUG test. To conduct a comprehensive assessment, we prioritize individual participants by offering additional support and addressing any challenges they may face throughout the testing process.

The TUG test is recorded from both the front and side views to assess the participants' performance thoroughly. A camera with a 1080p resolution and a frame rate of 30 frames per second is employed to guarantee the production of high-quality video. The data that has been collected comprises the MMU Parkinson Disease Dataset.

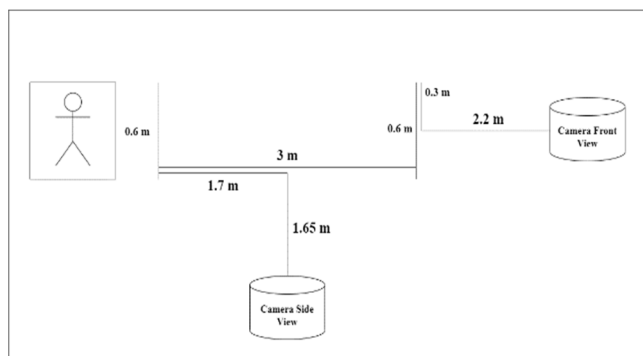


Fig. 2 TUG test setting

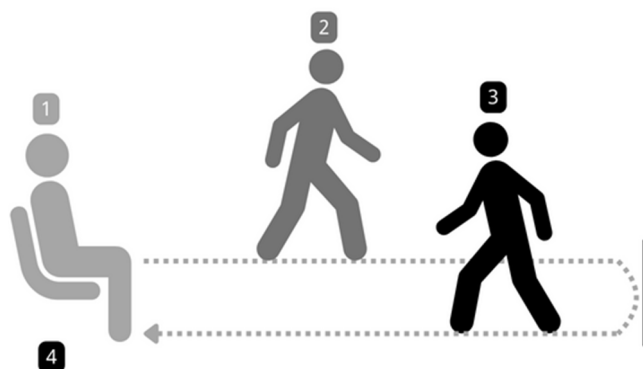


Fig. 3 TUG test example.

2) Video Enhancement:

Considering there are no restrictions set for the background during video collection, the recordings may include noise that may disrupt in further video processing steps. A script for improving videos was developed. This script utilizes the `alter_bg` package [15] to import a pre-trained PascalVOC model designed explicitly for modifying backgrounds. The `blur_video` function is then applied to add a moderate level of blur to the background, focusing on the recognized people inside the frames. This modification reduces the effect of background noise and results in a more accurate and visually distinct appearance for subsequent processing.

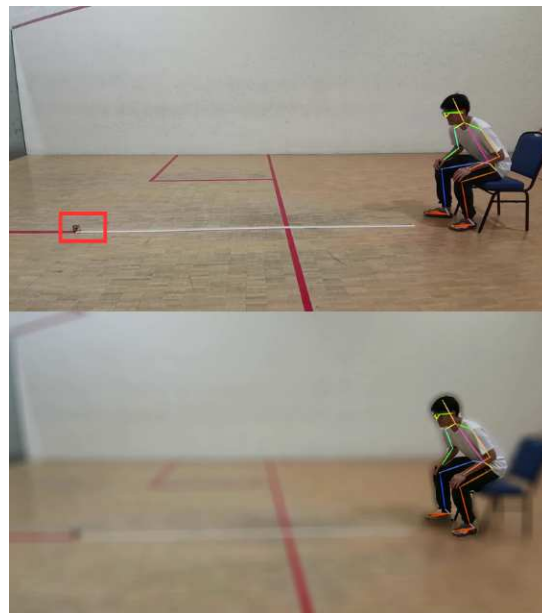


Fig. 4 AlphaPose plotting before and after video enhancement.

3) Body Key Points Estimation:

AlphaPose is applied to estimate the participant's body key point in this study. AlphaPose is a sophisticated method for estimating and tracking whole-body poses in multi-person scenarios [16]. It excels in real-time, local, and multi-person posture estimation tasks. It is an open-source solution that can produce high mean average precision (mAP) on benchmark datasets such as COCO. The capabilities of AlphaPose extend to applications in computer vision, human-computer interaction, and other domains that require exact human pose information. This study utilizes the model ZOO trained on the Halpe Full-Body Human Keypoints and HOI-Det dataset [16] to extract 26 key points related to the body movements, including nose, left eye, right eye, left ear, right ear, left shoulder, right shoulder, left elbow, right elbow, left wrist, right wrist, left hip, right hip, left knee, right knee, left ankle, right ankle, head, neck, hip, left big toe, right big toe, left small toe, right small toe, left heel, and right heel. The application of this model provides a more detailed information, particularly in the estimation of foot movements [16]. Fig. 5 presents a sample for body key points estimated by AlphaPose.

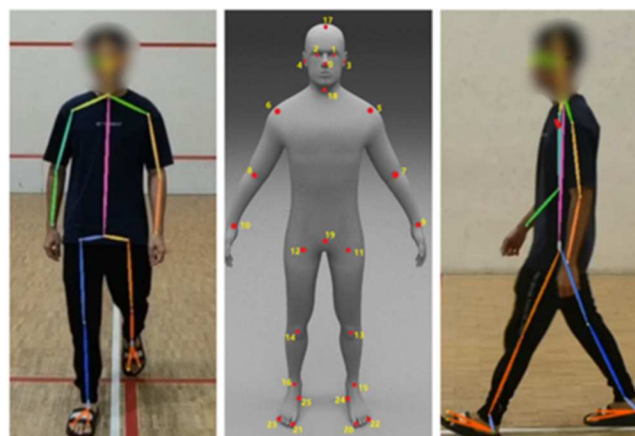


Fig. 5 Sample before and after AlphaPose Estimation.

4) Gait Signal Pre-Processing:

Signal Smoothing

In this study, a lowpass Butterworth filter [17] applied to the raw data to reduce noise and ensure smoother signal features:

$$f(x) = \frac{1}{1 + \left(\frac{x}{D}\right)^{2n}} \quad (1)$$

$f(s)$ is the transfer function of the filter.
 X is the complex frequency variable.
 D is the cutoff frequency.
 n is the filter order.

The implementation customizes filter parameters, such as cutoff frequency and order, based on the data's specific characteristics. The Nyquist frequency is a fundamental concept in digital signal processing, representing half of the sampling rate. It defines the maximum frequency that can be accurately represented in a digital signal. The cutoff frequency is the point at which the filter attenuates the signal. To design a filter, it's essential to express the cutoff frequency concerning the Nyquist frequency. This is done through the normalized cutoff frequency, calculated as $\text{cutoff_freq/nyquist}$. The smooth strength will increase with the normalized cut-off frequency.

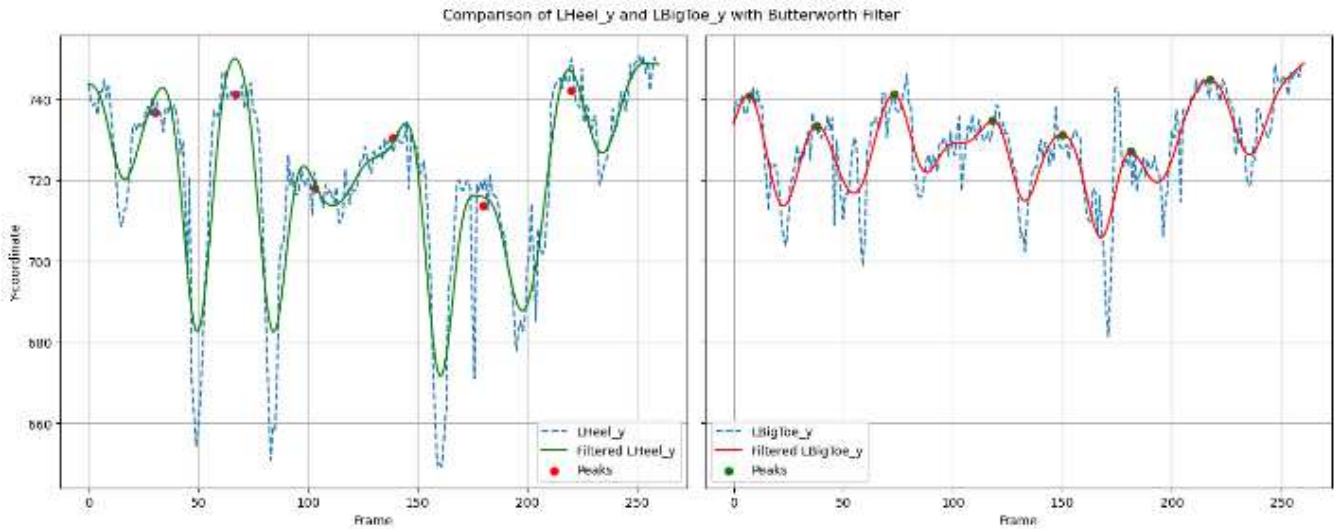


Fig. 6 Comparison between the y-coordinates signals for the Left Heel and Right Heel using smoothed data.

Class Balancing

In the context of an imbalanced dataset containing 28 subjects with varying distribution among three groups (12 young, 13 elderly, and 3 with PD), addressing the class imbalance issue is essential. Towards this end, random oversampler [18] is applied in this study [19], [20]. Random oversampling involves randomly duplicating instances from

the minority classes until the dataset is more balanced across all classes. Suppose x_i is a sample from the dataset, and its k nearest-neighbors x_{xi} are identified. By randomly selecting one of these neighbors and applying the random interpolation formula, a new sample x_{new} is generated those exhibits variations within the local neighborhood of x_i .

$$x_{new} = x_i + \lambda * (x_{xi} - x_i) \quad (2)$$

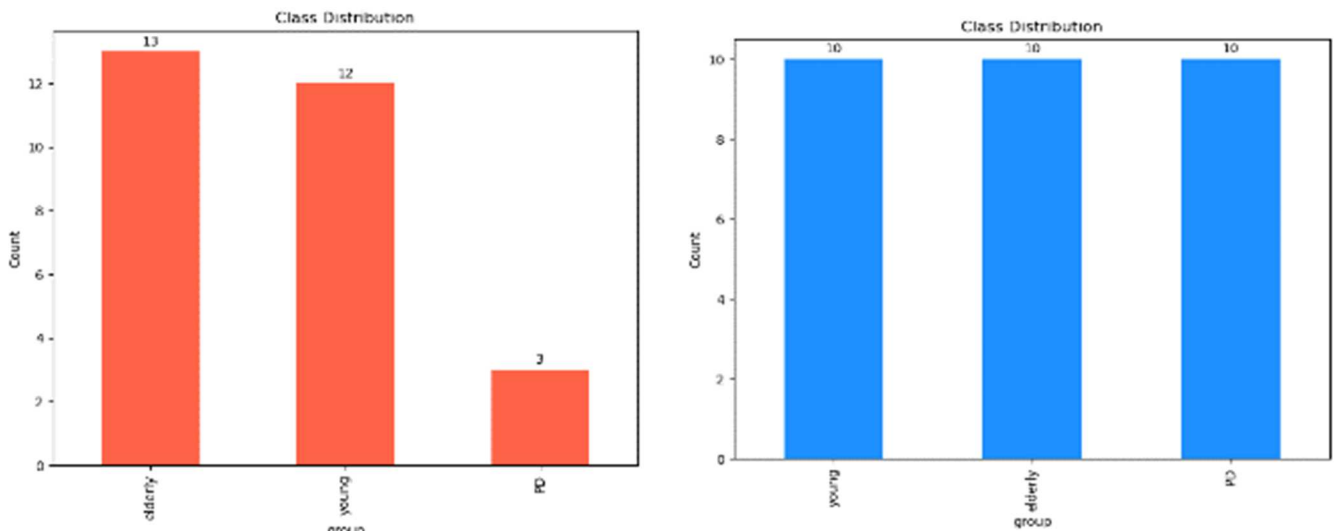


Fig. 7 Comparison of data before and after oversampling.

5) Turning Frame Extraction:

The primary goal of the Turning Frame Extraction process is to remove turning segments from the video, which are considered noise while retaining just the walking straight sections. The turning frame detection process includes the following steps:

- Calculate Shoulder Distance:** Compute the distance between the shoulders in each video frame.
- Graph Plotting:** Plot a graph using the shoulder distance data.
- Identify the Largest Distance:** Determine the frame with the largest shoulder distance, signifying a potential turning point.
- Locate Two Lowest Points:** Identify the two lowest points nearest to the shoulders in the graph.
- Define Turning Frame Range:** Determine the median of the two nearest lowest points and the highest point on the graph. This median serves as the turning frame range, marking the start and end of the turning segment.

These steps can be summarized by using the equation below:

$$\text{Turning Point} = - \left[\frac{|\text{HighestPeak} - \text{NearestTroughs}|}{2} \right] \quad (3)$$

Fig. 8 depicts the turning points detected in a walking sequence, and Fig. 9 shows a sample of the turning points detected in the video. The proposed turning frame detection technique efficiently separates the walking and turning phases in the video. Removing turning segments reduces noise and guarantees that future feature extraction focuses on meaningful walking data, which improves total analysis accuracy.

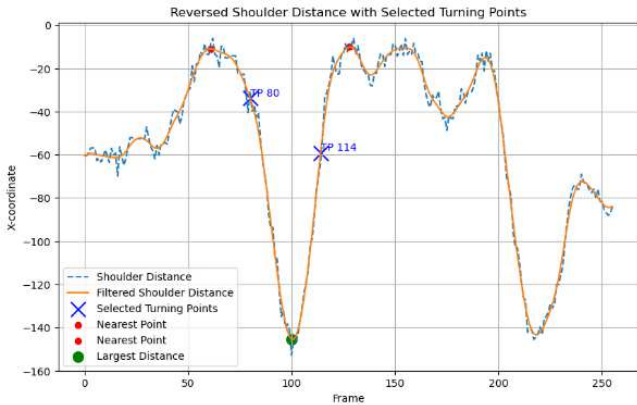


Fig. 8 Line graph to plot turning points.



Fig. 9 Video containing the plots for turning points.

6) Gait Cycle Identification:

In this study, the gait cycle is determined by identifying key events, such as heel strikes and toe-offs. The gait cycle is

typically divided into two phases: the stance phase and the swing phase, as shown in Fig. 10.

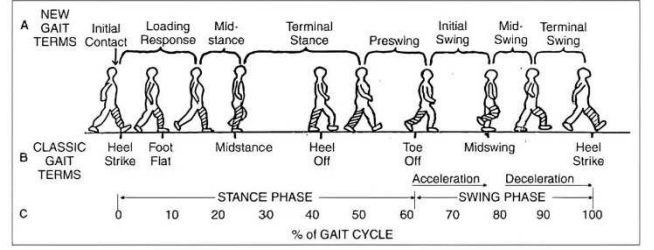


Fig. 10 Gait cycle phases

Table III summarizes the methods to extract the gait cycle. The gait cycle, representing a complete sequence of movements in human locomotion, can be defined and calculated using the following formula:

$$\text{Stride} = \text{HeelStrike}_j - \text{HeelStrike}_i \quad (4)$$

$$\text{Step} = \text{ToeOff} - \text{HeelStrike} \quad (5)$$

Here, the stride refers to a complete gait cycle, encompassing one full sequence of steps involving both the left and right limbs. Alternatively, a step can denote half of a gait cycle, focusing on the movement of one limb left during walking.

TABLE III
METHODS TO EXTRACT GAIT CYCLE.

Steps	Descriptions
Identify Heel Strikes and Toe-Offs	<ul style="list-style-type: none"> Heel strikes occur when the heel contacts the ground. Toe-offs occur when the toe leaves the ground.
Peak Detection	a. Apply a threshold to the signal to filter out noise and identify significant peaks representing gait events.
Thresholding	b. Apply a threshold to the signal to filter out noise and identify significant peaks representing gait events.

7) Feature Extraction:

In this section, gait features are extracted from the gait cycle to facilitate model training. The following formula is used to compute these gait features [21], [22], [23]. To find the Euclidean distance $DE_{E(i,j)}$ between two points, the formula applied is:

$$D_{E(i,j)} = \left[(x_i - x_j)^2 + (y_i - y_j)^2 \right]^{\frac{1}{2}} \quad (6)$$

- Stance time: The amount of time one foot is on the ground during a gait cycle.

$$\text{Stance}_T = \frac{\text{ToeOff}_i - \text{HeelStrike}_i}{\text{FPS used}} \quad (7)$$

- Swing time: The amount of time one foot spends in the air during a gait cycle.

$$\text{Swing}_T = \frac{\text{HeelStrike}_j - \text{ToeOff}_i}{\text{Video FPS}} \quad (8)$$

- Step length: The distance between two consecutive heel strikes of the same foot.

$$\text{Step}_L = \text{Mean } D_E(\text{LHeelStrike}, \text{RHeelStrike}) \quad (9)$$

d. Step time: The total time taken to complete one step.

$$Step_T = \frac{ToeOff_j - HeelStrike_i}{Video\ FPS} \quad (10)$$

e. Stride length: The horizontal distance between two consecutive heel strikes of the same foot.

$$Stride_T = Mean D_E(HeelStrike_j, HeelStrike_i) \quad (11)$$

f. Stride time: The total time taken to complete one entire gait cycle.

$$Stride_T = \frac{HeelStrike_j - HeelStrike_i}{Video\ FPS} \quad (12)$$

g. Cadence: The number of steps per unit of time.

$$Cadence = \frac{Number\ of\ steps}{Time\ used\ (minutes)} \quad (13)$$

h. Speed: The rate of motion.

$$Speed = Number\ of\ Step \times cadence \quad (14)$$

III. RESULTS AND DISCUSSION

This section discusses the experiments conducted to evaluate the performance of the proposed PD detection methods.

A. Data Exploration

The correlation heat map shown in Fig. 11 offers a visual insight into the dataset's relationships between various gait features. Each cell in the map represents the correlation coefficient between two variables, with the color intensity indicating the strength and direction of the correlation. Warmer colors typically signify a positive correlation, while cooler colors depict a negative correlation [24]. This graph helps identify patterns of association or disassociation between variables, which can reveal potential dependencies within the dataset.

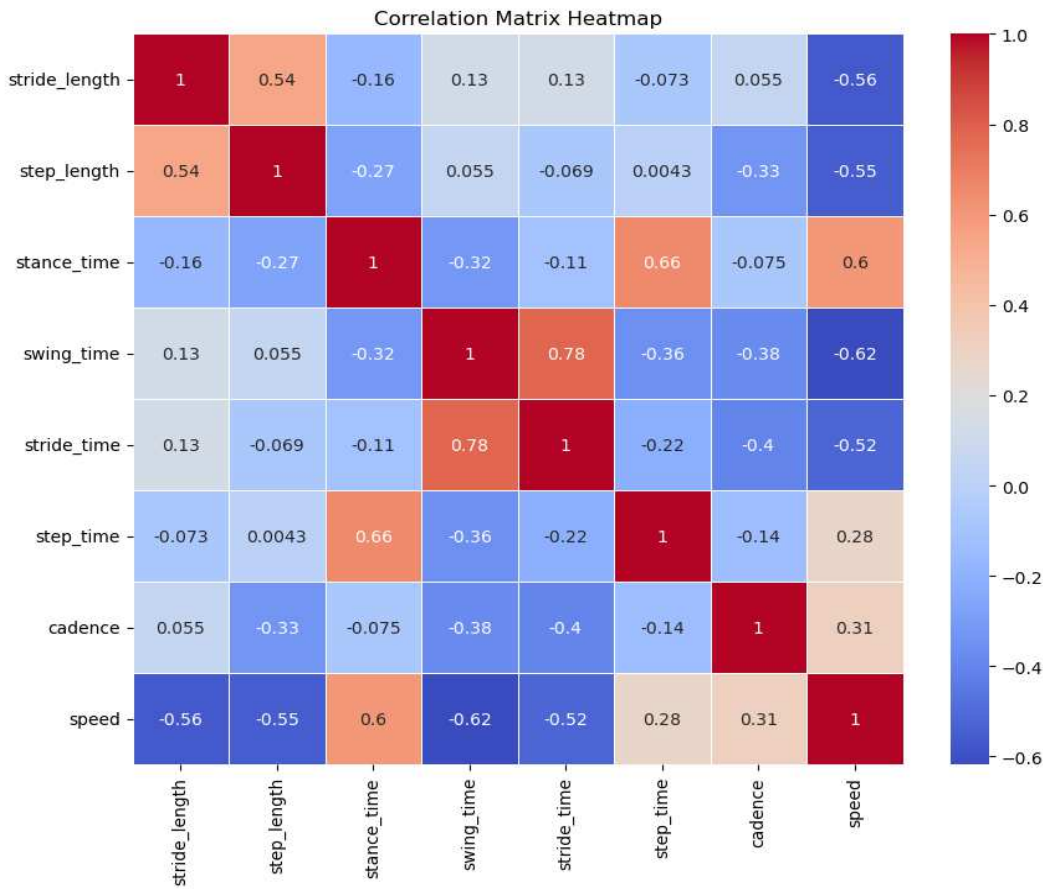


Fig. 11 Correlation matrix heatmap of the gait features.

The bar plots in Fig. 12 compare the average values among young adults, elderly individuals, and those with PD, focusing on metrics such as step length, step time, stride length, stride time, stance time, swing time, cadence, and speed. The analysis determines trends in these feature values across the three groups. We observe generally consistent trends of

increase or decrease from young adults to the elderly to those with PD. For instance, increased stride or step length across these groups suggests a positive trend. Conversely, a decrease in metrics like speed and cadence indicates a negative correlation [25].

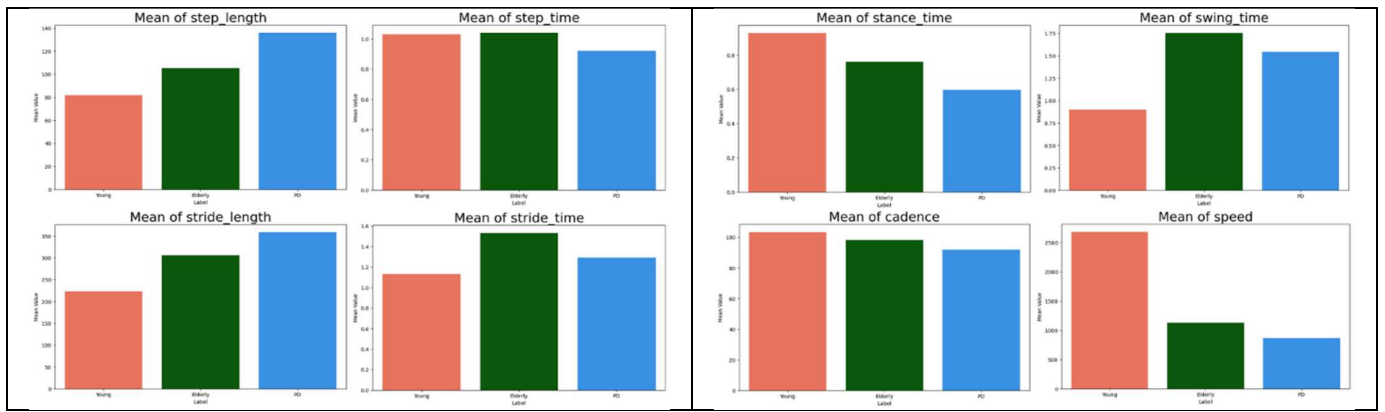


Fig. 12 Comparison of average feature values between different participant groups.

B. Classification and Performance Evaluation

In the classification task, we employed Support Vector Machine (SVM) [26] and CatBoost models [27] on a dataset divided into 80% for training and 20% for testing [28], [29]. Both models demonstrated comparable performance metrics, as shown in Table IV. Fig. 13 and Fig. 14 provide graphical comparisons between the two methods regarding accuracy and confusion matrices.

TABLE IV
PERFORMANCE COMPARISON OF SVM AND CATBOOST

Classifier	Accuracy (%)	Precision (%)	Recall (%)	F1 Score (%)
SVM	83.33	83.33	83.33	78.00
CatBoost	83.33	83.33	83.33	78.00

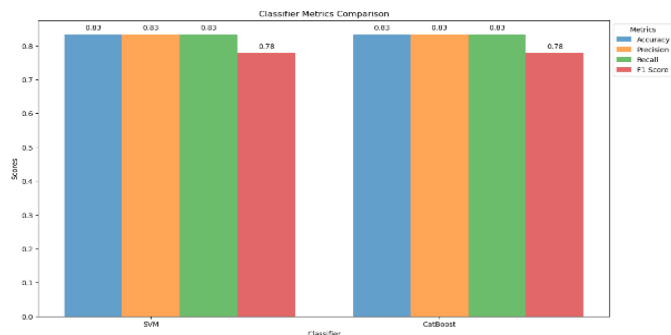


Fig. 13 Performance comparison of SVM and CatBoost

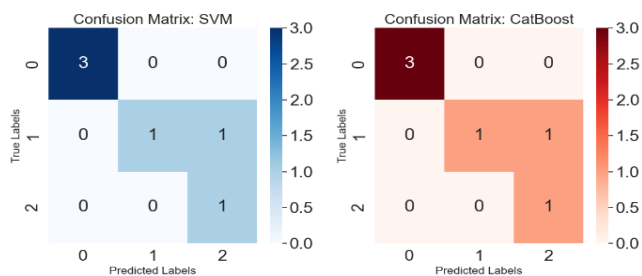


Fig. 14 Comparison of confusion matrix between SVM and Cat Boost.

Overall, we observe that the high frequency of temporal gait metrics such as stance time, stride time, and step time highlights their importance in discriminating across groups in the dataset. Notably, the difference in feature significance between SVM and CatBoost demonstrates the distinctive modeling methods and criteria used by each algorithm in reaching classification decisions.

C. Investigating Features Importance

In this section, we further explore which features are essential in the SVM and CatBoost models and how they relate to PD [30]. The SVM model shows that step, stride, and stance time are the three most important characteristics (see Fig. 15). Stance time is the duration a foot is in contact with the ground during a walking cycle. It provides a strong indicator of balance problems and muscle stiffness commonly found in people with PD. Stride time measures the period between the heel strikes of the same foot in succession. It helps predict changes in walking speed and rhythm related to motor deficits seen in PD, such as slow movement. Step time measures the duration of a single step and highlights the timing irregularities in walking patterns characteristic of a Parkinsonian gait.

On the other hand, the CatBoost model identifies stride length, speed, and stride time as critical for classification (Fig. 16) [31]. Stride length's relevance stems from its ability to reflect gait regularity and rhythm disturbances that are symptomatic of PD-related motor difficulties. Individuals with PD often exhibit shorter strides due to challenges in initiating and maintaining movement. Walking speed, influenced by both motor and cognitive impairments, is a significant indicator of Parkinsonian gait, characterized by slower movements and diminished motor control.

These characteristics are essential for measuring and understanding the unique walking patterns connected to PD. The focus on temporal (stance time, stride time, step time) and spatial (stride length, speed) gait parameters highlights their potential clinical utility as biomarkers for Parkinson's disease (PD) diagnosis, tracking the course of the disease, and leading targeted measures meant to enhance mobility and quality of life [32].

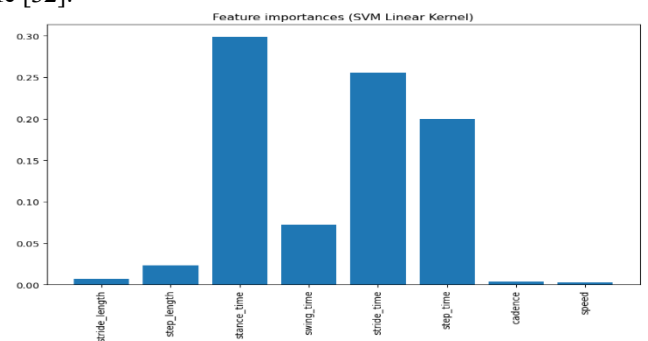


Fig. 15 Feature importance determined by SVM.

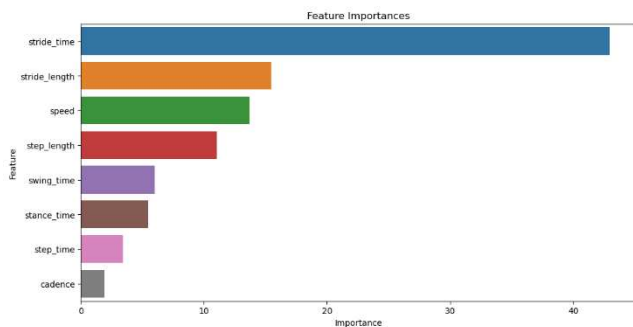


Fig. 16 Feature importance derived from CatBoost.

D. Findings

The following are some exciting findings from this study: The SVM and CatBoost models perform well predicting PD, with an average accuracy of 83.33%. Important features related to PD prediction have been discovered, providing insight into the different gait factors determining stance time and speed. We observe that PD patients have lower speeds and stance times. These findings help to classify people with PD more effectively.

IV. CONCLUSION

The study proposes a comprehensive approach for using computer vision and machine learning to perform PD recognition. The MMU Parkinson Disease Dataset is constructed to enable the analysis of patterns in gait dynamics. In the classification phase, the Support Vector Machine (SVM) and CatBoost models performed well, with an excellent accuracy score of 83.33%. Lower speed and stance time were identified as recognized symptoms for Parkinson's disease, providing valuable insights into future detection approaches. However, it is essential to realize the study's limitations, especially those caused by a limited dataset and the need to explore possible gait features further. Overcoming these constraints is critical to improve the accuracy of PD detection.

In conclusion, this study contributes to existing research in Parkinson's disease detection by combining demonstrated methodology with innovative methods. The findings emphasize the importance of gait patterns in PD and identify specific features required for appropriate classification. As the research ends, the call to action remains: increase datasets, proceed deeper into feature investigation, and aim for constant progress in enhancing PD detection.

Future research must focus on collecting extensive and varied datasets, utilizing advanced feature extraction techniques, incorporating multimodal data, and validating models in real-world scenarios. These efforts will help with early detection and monitoring of PD, ultimately enhancing patient results and disease control.

ACKNOWLEDGMENT

This work was partly supported by research grants from the Fundamental Research Grant Scheme (FRGS) (FRGS/1/2020/ICT02/MMU/02/5) and the MMU-ZUJ International Matching Grant.

REFERENCES

- [1] Z. Ou et al., "Global Trends in the Incidence, Prevalence, and Years Lived With Disability of Parkinson's Disease in 204 Countries/Territories From 1990 to 2019," *Frontiers in Public Health*, vol. 9, Dec. 2021, doi: 10.3389/fpubh.2021.776847.
- [2] F. C. Church, "Treatment Options for Motor and Non-Motor Symptoms of Parkinson's Disease," *Biomolecules*, vol. 11, no. 4, p. 612, Apr. 2021, doi: 10.3390/biom11040612.
- [3] O. Escamilla-Luna, M. A. Wister, and J. Hernandez-Torruco, "Classification Algorithms for Analyzing Parkinson's Disease Patient," *2022 International Conference on Software, Telecommunications and Computer Networks (SoftCOM)*, vol. 3, pp. 1–6, Sep. 2022, doi: 10.23919/softcom55329.2022.9911391.
- [4] J. Ajay, C. Song, A. Wang, J. Langan, Z. Li, and W. Xu, "A pervasive and sensor-free Deep Learning system for Parkinsonian gait analysis," *2018 IEEE EMBS International Conference on Biomedical & Health Informatics (BHI)*, vol. 12, pp. 108–111, Mar. 2018, doi: 10.1109/bhi.2018.8333381.
- [5] C. Urcuqui et al., "Exploring Machine Learning to Analyze Parkinson's Disease Patients," *2018 14th International Conference on Semantics, Knowledge and Grids (SKG)*, vol. 18, pp. 160–166, Sep. 2018, doi: 10.1109/skg.2018.00029.
- [6] Y. Liu et al., "Vision-Based Method for Automatic Quantification of Parkinsonian Bradykinesia," *IEEE Transactions on Neural Systems and Rehabilitation Engineering*, vol. 27, no. 10, pp. 1952–1961, Oct. 2019, doi: 10.1109/tnsre.2019.2939596.
- [7] J.-S. Seo, Y. Chen, D.-Y. Kwon, and C. Wallraven, "Single-view, video-based diagnosis of Parkinson's Disease based on arm and leg joint tracking," *2022 International Conference on Mechanical, Automation and Electrical Engineering (CMAEE)*, vol. 08792, pp. 172–176, Dec. 2022, doi: 10.1109/cmaee58250.2022.00037.
- [8] B. E., B. D., V. K. Elumalai, and V. R., "Automatic and non-invasive Parkinson's disease diagnosis and severity rating using LSTM network," *Applied Soft Computing*, vol. 108, p. 107463, Sep. 2021, doi: 10.1016/j.asoc.2021.107463.
- [9] J. Prince and M. de Vos, "A Deep Learning Framework for the Remote Detection of Parkinson's Disease Using Smart-Phone Sensor Data," *2018 40th Annual International Conference of the IEEE Engineering in Medicine and Biology Society (EMBC)*, Jul. 2018, doi: 10.1109/embc.2018.8512972.
- [10] T. Li et al., "Automatic Timed Up-and-Go Sub-Task Segmentation for Parkinson's Disease Patients Using Video-Based Activity Classification," *IEEE Transactions on Neural Systems and Rehabilitation Engineering*, vol. 26, no. 11, pp. 2189–2199, Nov. 2018, doi: 10.1109/tnsre.2018.2875738.
- [11] J. F. Reyes, J. Steven Montealegre, Y. J. Castano, C. Urcuqui, and A. Navarro, "LSTM and Convolution Networks exploration for Parkinson's Diagnosis," *2019 IEEE Colombian Conference on Communications and Computing (COLCOM)*, Jun. 2019, doi: 10.1109/colcomcon.2019.8809160.
- [12] M. D. Hssayeni, J. L. Adams, and B. Ghoraani, "Deep Learning for Medication Assessment of Individuals with Parkinson's Disease Using Wearable Sensors," *2018 40th Annual International Conference of the IEEE Engineering in Medicine and Biology Society (EMBC)*, pp. 1–4, Jul. 2018, doi: 10.1109/embc.2018.8513344.
- [13] S. Caramaschi et al., "A Smartphone-Based Timed Up and Go Test for Parkinson's Disease," *Pervasive Computing Technologies for Healthcare*, pp. 515–519, 2024, doi: 10.1007/978-3-031-59717-6_34.
- [14] K. Dunning, "Timed Up and Go Test," *Encyclopedia of Clinical Neuropsychology*, pp. 1–2, 2017, doi: 10.1007/978-3-319-56782-2_1969-2.
- [15] P. Virtanen et al., "SciPy 1.0: fundamental algorithms for scientific computing in Python," *Nature Methods*, vol. 17, no. 3, pp. 261–272, Feb. 2020, doi: 10.1038/s41592-019-0686-2.
- [16] H.-S. Fang et al., "AlphaPose: Whole-Body Regional Multi-Person Pose Estimation and Tracking in Real-Time," *IEEE Transactions on Pattern Analysis and Machine Intelligence*, vol. 45, no. 6, pp. 7157–7173, Jun. 2023, doi: 10.1109/tpami.2022.3222784.
- [17] SciPy, "scipy.signal.butter — SciPy v1.13.0 Manual." Accessed: Apr. 09, 2024. [Online]. Available: <https://docs.scipy.org/doc/scipy/reference/generated/scipy.signal.butter.html>.
- [18] Random Over Sampler, "RandomOverSampler — Version 0.12.2." Accessed: Apr. 09, 2024. [Online]. Available: https://imbalanced-learn.org/stable/references/generated/imblearn.over_sampling.RandomOverSampler.html.

- [19] C. Yang, E. A. Fridgerisson, J. A. Kors, J. M. Reys, and P. R. Rijnbeek, "Impact of random oversampling and random undersampling on the performance of prediction models developed using observational health data," *Journal of Big Data*, vol. 11, no. 1, Jan. 2024, doi: 10.1186/s40537-023-00857-7.
- [20] T. Wongvorachan, S. He, and O. Bulut, "A Comparison of Undersampling, Oversampling, and SMOTE Methods for Dealing with Imbalanced Classification in Educational Data Mining," *Information*, vol. 14, no. 1, p. 54, Jan. 2023, doi: 10.3390/info14010054.
- [21] T. Connie, T. B. Aderinola, T. S. Ong, M. K. O. Goh, B. Erfianto, and B. Purnama, "Pose-Based Gait Analysis for Diagnosis of Parkinson's Disease," *Algorithms*, vol. 15, no. 12, p. 474, Dec. 2022, doi: 10.3390/a15120474.
- [22] X. L. Lau, T. Connie, M. K. O. Goh, and S. H. Lau, "Fall Detection and Motion Analysis Using Visual Approaches," *International Journal of Technology*, vol. 13, no. 6, p. 1173, Nov. 2022, doi: 10.14716/ijtech.v13i6.5840.
- [23] V. Rani and M. Kumar, "Human gait recognition: A systematic review," *Multimedia Tools and Applications*, vol. 82, no. 24, pp. 37003–37037, Mar. 2023, doi: 10.1007/s11042-023-15079-5.
- [24] D. Zhu, L. Ji, L. Zhu, and C. Li, "Gait coordination feature modeling and multi-scale gait representation for gait recognition," *International Journal of Machine Learning and Cybernetics*, vol. 15, no. 9, pp. 3791–3802, Apr. 2024, doi: 10.1007/s13042-024-02120-8.
- [25] X. Zhang et al., "The impact of anxiety on gait impairments in Parkinson's disease: insights from sensor-based gait analysis," *Journal of NeuroEngineering and Rehabilitation*, vol. 21, no. 1, Apr. 2024, doi: 10.1186/s12984-024-01364-3.
- [26] A. J. Smola and B. Schölkopf, "A tutorial on support vector regression," *Statistics and Computing*, vol. 14, no. 3, pp. 199–222, Aug. 2004, doi: 10.1023/b:stco.0000035301.49549.88.
- [27] CatBoost, "CatBoost - open-source gradient boosting library." Accessed: Apr. 09, 2024. [Online]. Available: <https://catboost.ai/>.
- [28] A. A. Ibrahim, R. L., M. M., R. O., and G. A., "Comparison of the CatBoost Classifier with other Machine Learning Methods," *International Journal of Advanced Computer Science and Applications*, vol. 11, no. 11, 2020, doi: 10.14569/ijacsa.2020.0111190.
- [29] A. Villar and C. R. V. de Andrade, "Supervised machine learning algorithms for predicting student dropout and academic success: a comparative study," *Discover Artificial Intelligence*, vol. 4, no. 1, Jan. 2024, doi: 10.1007/s44163-023-00079-z.
- [30] L. di Biase et al., "Gait Analysis in Parkinson's Disease: An Overview of the Most Accurate Markers for Diagnosis and Symptoms Monitoring," *Sensors*, vol. 20, no. 12, p. 3529, Jun. 2020, doi: 10.3390/s20123529.
- [31] M. Al-Sarem, F. Saeed, W. Boulila, A. H. Emara, M. Al-Mohaimeed, and M. Errais, "Feature Selection and Classification Using CatBoost Method for Improving the Performance of Predicting Parkinson's Disease," *Advances on Smart and Soft Computing*, pp. 189–199, Oct. 2020, doi: 10.1007/978-981-15-6048-4_17.
- [32] S. Das, G. Kothari, A. Prakash, A. J. D. Krupa, Samiappan, and Dhanalakshmi, "Machine learning approaches in detection of Parkinson's disease using speech and gait signals," *Contemporary Innovations In Engineering And Management*, vol. 2821, p. 070006, 2023, doi: 10.1063/5.0150531.